Published in final edited form as:
Biomaterials. 2009 September ; 30(27): 4618–4628. doi:10.1016/j.biomaterials.2009.05.030.

The Phosphorylation of Vascular Endothelial Growth Factor Receptor-2 (VEGFR-2) by Engineered Surfaces with Electrostatically or Covalently Immobilized VEGF

Sean M. Anderson[1], **Tom T. Chen**[2], **M. Luisa Iruela-Arispe**[2], and **Tatiana Segura**[1,*]

[1]University of California, Los Angeles, Chemical and Biomolecular Engineering Department, Los Angeles, CA

[2]University of California, Los Angeles, Molecular, Cellular, and Developmental Biology Department, Los Angeles, CA

Abstract

Growth factors are a class of signaling proteins that direct cell fate through interaction with cell surface receptors. Although a myriad of possible cell fates stem from a growth factor binding to its receptor, the signaling cascades that result in one fate over another are still being elucidated. One possible mechanism by which nature modulates growth factor signaling is through the method of presentation of the growth factor – soluble or immobilized (matrix bound). Here we present the methodology to study signaling of soluble versus immobilized VEGF through VEGFR-2. We have designed a strategy to covalently immobilize VEGF using its heparin-binding domain to orient the molecule (bind) and a secondary functional group to mediate covalent binding (lock). This bind-and-lock approach aims to allow VEGF to assume a bioactive orientation before covalent immobilization. Surface plasmon resonance (SPR) demonstrated heparin and VEGF binding with surface densities of 60 ng/cm^2 and 100 pg/cm^2, respectively. ELISA experiments confirmed VEGF surface density and showed that electrostatically bound VEGF releases in cell medium and heparin solutions while covalently bound VEGF remains immobilized. Electrostatically bound VEGF and covalently bound VEGF phosphorylate VEGFR-2 in both VEGFR-2 transfected cells and VEGFR-2 endogenously producing cells. HUVECs plated on VEGF functionalized surfaces showed different morphologies between surface-bound VEGF and soluble VEGF. The surfaces synthesized in these studies allow for the study of VEGF/VEGFR-2 signaling induced by covalently bound, electrostatically bound, and soluble VEGF and may provide further insight into the design of materials for the generation of a mature and stable vasculature.

Keywords

Angiogenesis; Cell Signaling; Endothelial Cell; Fibronectin; Growth Factors; Heparin

*Corresponding Author Tatiana Segura, 420 Westwood Plaza, 5531 Boelter Hall, Los Angeles, CA, 90095, tsegura@ucla.edu.

Introduction

Tissue engineering and tissue regeneration approaches presently suffer from oxygen and nutrient delivery constraints because of the inability of current scaffolds to guide the formation of stable and long lasting vascular networks (1). Cells seeded or residing in the middle of the tissue construct have a limited supply of oxygen and nutrients since blood vessels are not infiltrating at an appreciable rate, and the diffusion limit of oxygen is only a few hundred microns (2). Vascular endothelial growth factor (VEGF) is a key component in the signaling cascade to form new blood vessels from existing vessels and can trigger proliferation, migration, and survival of cells through a single growth factor-receptor binding event (3). Because of alternative splicing, VEGF can exist as many different isoforms with different affinities for the extracellular matrix (ECM). For example, $VEGF_{165}$ binds to the ECM while $VEGF_{121}$ remains soluble. $VEGF_{165}$ contains a 55 amino acid long heparin-binding domain located at the C-terminus end of the protein and is coded by exons 6 and 7 of the VEGF gene (4). The affinity of VEGF for the ECM has been shown to regulate angiogenesis and the morphology of the blood vessels formed. In prostate cancer, the ratio of $VEGF_{121}$/$VEGF_{165–189}$ increases as tumor angiogenesis increases (5) and the enhanced release of $VEGF_{165}$ from the ECM by matrix metalloproteinases and plasmid has been shown to increase angiogenesis in colorectal cancer (6). Further, VEGF immobilized to three dimensional matrices leads to the formation of smaller, structured capillary networks, while encapsulated (soluble) $VEGF_{165}$ leads to the formation of large, leaky blood vessels *in vivo* (1,7,8). Last, $VEGF_{165}$ that is immobilized in two dimensions shows enhanced endothelial cell proliferation and migration *in vitro* (9–12).

Differences in cell biology as a result of cells being in contact with soluble *versus* immobilized growth factors are not unique to VEGF. Studies using immobilized epidermal growth factor (EGF) and nerve growth factor (NGF) show different cellular behavior for immobilized and soluble growth factors (13,14). Further, studies with covalently immobilized EGF to cell culture substrates via a tresyl chloride mediated binding have shown that the growth factor is still able to phosphorylate the EGF receptor (14), suggesting that receptor internalization is not needed to activate the receptor and induce downstream signaling. The ability to phosphorylate cell surface receptors from covalently immobilized cytokines was also observed between epoxy immobilized Granulocyte Macrophage Colony Stimulating Factor (GM-CSF) and its receptor, STAT5 (15).

Protein immobilization has been investigated through the use of unspecific chemistry such as amine/carboxylic acid chemistry (9,16,17) and thiol chemistry (18), or through the use of biological interactions such as biotin-avidin (19). However, these approaches result in the immobilized protein being bound through different conformations on the surface and result in reduction of protein activity (20). Approaches to immobilize proteins with uniform orientation typically involve the engineering and production of the protein using recombinant techniques to introduce ligands for specific receptors (10,20) or functional groups such as thiols at specific locations in the protein (21). Alternatively, the natural affinity of growth factors for the extracellular matrix, especially heparin binding, has been exploited to electrostatically bind growth factors to natural (22,23) or synthetic (24–26) hydrogels and to heparin modified hydrogels and surfaces (22,23,26,27). Heparin binding has the advantage that the protein does not have to be modified and that the natural binding affinity of the growth factor for the ECM can be exploited. Immobilization of proteins to glass through silane chemistry (28) or gold through self-assembled monolayers (SAMs) (20,29–31) has been extensively used with the above-mentioned strategies. Gold substrates are especially attractive for protein immobilization because SAM forming thiols are available with a variety of functional groups and the quantification of the immobilized molecules, polymers, and proteins can be characterized using Surface Plasmon Resonance (SPR).

Although studies have begun to point out the differences in cellular behavior due to the affinity of $VEGF_{165}$ (referred to as VEGF from now on) for the ECM, strategies to compare VEGFR-2 phosphorylation and downstream signaling as a function of the affinity of VEGF for the matrix are not available. Our objective in this report was to synthesize surfaces that contained either electrostatically or covalently bound VEGF and to determine if covalently immobilized VEGF was able to phosphorylate VEGFR-2. Our strategy to immobilize VEGF takes advantage of the heparin-binding domain at the C-terminus of the protein to orient the growth factor on the surface and a photoreactive group to covalently bind the growth factor to the surface in that orientation (bind-and-lock approach, Figure 1). Heparin was oxidized, modified with a photoreactive group, and immobilized to an amine containing SAM on gold surface through reductive amination. VEGF was then allowed to electrostatically bind to the heparin-modified surface and then the surface was exposed to UV light to covalently immobilize (lock) the growth factor into place. Heparin without the photoreactive group was used as a control, which resulted in VEGF that was only electrostatically bound through its heparin-binding domain. For cellular experiments, fibronectin (FN) was used to backfill the surface. This approach offers the ability to study VEGF signaling using VEGF that has three different affinities for the ECM - covalent (high), electrostatic (medium) and soluble (low).

Materials and Methods

Materials

(1-Mercapto-11-undecyl) tetra (ethylene glycol) (EG-OH) was purchased from Asemblon (Redmond, WA). (1-Mercapto-11-undecyl) septa (ethylene glycol) amine ($EG\text{-}NH_2$) was obtained from ProChimia (Evanston, IL). Heparin sodium salt from porcine intestinal mucosa was purchased from Alfa Aesar (Ward Hill, MA). Vascular Endothelial Growth Factor (VEGF) was purchased from Shenandoah Biotechnology (Warwick, PA). Porcine aortic endothelial (PAE/KDR) cells overexpressing KDR, the human isoform of VEGFR-2, were provided by Dr. Gera Neufeld of Technicon, Israel. Human umbilical vein endothelial cells (HUVEC) were a kind gift from Dr. Andy Putnam of UC Irvine. All other reagents and products were purchased from Fisher Scientific unless noted otherwise.

Cell culture

PAE/KDR cells were cultured in F-12 (Invitrogen, Grand Island, NY) medium supplemented with 10% bovine growth serum (BGS, Hyclone, Logan, Utah) and 1% penicillin/streptomycin (Invitrogen, Grand Island, NY) at 37°C and 5% CO_2. HUVECs were cultured in EGM-2 complete medium (Lonza, Basel, Switzerland) at 37°C and 5% CO_2. Both cell types were split using trypsin following standard protocols and were typically used up to passage 10.

Heparin-ABH synthesis

Heparin was modified with the photoreactive group p-azidobenzoyl by first oxidizing heparin using sodium periodate ($NaIO_4$) to introduce aldehyde groups throughout the heparin backbone and then reacting the oxidized heparin with a heterobifunctional crosslinker that reacts with aldehydes on one end and contains the photoreactive group on the other end. Heparin (62.5 mg/mL) was mixed with a solution of $NaIO_4$ (200 mM) in 100 mM sodium acetate buffer (pH 5) and incubated for 2 days at 4°C to allow the reaction to occur. The reaction mixture was purified through dialysis (3500 MWCO), lyophilized and stored as a powder at 4°C until used. Oxidized heparin (3 mg/mL) was mixed with p-azidobenzoyl hydrazide (ABH, Pierce, Rockford, IL, 0.65 mM) in PBS buffer (pH 7.4) for 2 hours and the reaction mixture purified through dialysis. The final product was lyophilized and stored as a powder at 4°C in the dark. Oxidized heparin was characterized through infrared spectra using an FTIR spectrometer (Jasco FT/IR-420). Heparin-ABH was characterized through UV absorbance at 290 nm in a Beckman Coulter DU 730 (Fullerton, CA).

Gold evaporation and Self Assembled Monolayer (SAM) formation

Gold substrates were generated by e-beam evaporation resulting in 30 nm thick gold on a 5 nm titanium adhesion layer over standard laboratory glass slides following a piranha clean. Gold substrates were cleaned once with acetone and twice with sterile 200 proof ethanol, dried under argon or nitrogen, and immersed in a 2 mM solution of 1% EG-NH_2 and 99% EG-OH for 18 hours. Following the incubation, the gold substrates were washed with ethanol twice and dried under argon or nitrogen. Contact angle and ellipsometry measurements were obtained to verify SAM formation and stability against long wave UV light. Contact angles were measured using a goniometer (Newport VPH-2, First Ten Angstroms, Inc.) and ellipsometry measurements were taken with a SopraGES5 ellipsometer (Palo Alto, CA).

Heparin and VEGF Immobilization

Heparin-ABH was immobilized to an amine containing SAM surface through the formation of a Schiff base between the aldehyde groups in heparin and the amines on the SAM surface, followed by reductive amination to form an irreversible bond. Heparin-ABH (1 mg/ml) was incubated on a 1% EG-NH_2 SAM surface for 24 hours at 4°C, followed by a sodium cyanoborohydride incubation (50 mM in 100 mM sodium acetate pH 4) for 5 minutes at room temperature. The remaining aldehydes on the immobilized oxidized heparin were quenched with 500 mM TRIS (pH 8) for 10 minutes at room temperature, followed by another sodium cyanoborohydride 5 minute incubation. The heparin modified surfaces were then washed two times with 0.05% Tween-20 in PBS and two times with PBS to remove non-specifically bound heparin and immediately used to immobilize VEGF. Heparin modified SAM surfaces were incubated with VEGF (200 ng/mL in PBS) for 24 hours at 4°C, washed with PBS, and exposed to UV light (365 nm, UVL-54, UVP, Upland, CA) for 10 minutes. The resulting VEGF modified surfaces were washed three times with 0.05% Tween-20 in PBS and incubated for up to 2 days in a heparin containing solution (1 mg/ml heparin in 0.05% Tween-20 in PBS) at 4°C to release all non-specifically bound VEGF, followed by a PBS wash. VEGF surfaces that did not contain ABH were formed following the same protocol, but oxidized heparin was used instead of heparin-ABH and 0.05% Tween-20 in PBS was used for the release step rather than the heparin solution. All surfaces were immediately used.

Heparin and VEGF binding density analysis

A Biacore T100 Molecular Interaction System (GE, Amersham Biosciences, Pittsburgh, PA) was used to characterize the binding of heparin and VEGF to amine functionalized surfaces. 1 cm × 1.2 cm gold chips were purchased from Biacore and functionalized to form 1% EG-NH_2 SAMs as described above. The surfaces were primed with filtered PBS (pH 7.4) and the baseline was allowed to stabilize at 5 μl/min. Oxidized heparin (1 mg/ml) was injected at 5 μl/min for 30 min followed by sodium cyanoborohydride (100 mM) in 100 mM sodium acetate (pH 4) at 5 μl/min for 7 min. TRIS buffer (100 mM, pH 8) was subsequently injected at 5 μl/min for 6 min. Two 0.05% Tween-20 in PBS (pH 7.4) injections at 5 μl/min for 5 min each were used as washes. VEGF (200 ng/ml) was injected at 5 μl/min for 15 min. Between injections and after the final injection, the signal was allowed to stabilize for 5–10 min with continuous flow of filtered PBS (pH 7.4) at 5 μl/min.

Cellular characterization of the surface

Cell attachment and spreading on the surface was used to study the protein adsorption properties of the surface. Human plasma fibronectin (Sigma-Aldrich, Saint Louis, MO) was incubated on the SAM surface (100% EG-OH or 1% EG-NH_2, with and without heparin) at 20 μg/ml for 2 h at 4°C followed by a 30 min 1% BSA-PBS block step. PAE/KDR cells were plated without serum at 500,000 cells/ml for 20 min for the attachment assay and allowed to spread for 2 h for the spreading assay. After the experiment was complete, the cells were washed

with PBS and fixed with 4% paraformaldehyde. Following 0.1% Triton X-100 treatment and a 1% BSA blocking step, the cells were incubated with HOESCHT and phalloidin Alexa 488 (Invitrogen, Carlsbad, CA). Images were acquired on a Zeiss microscope and quantified with ImageJ software by counting cells and analyzing their spread area with the tracer function.

VEGF release kinetics and surface quantification

To quantify the release kinetics of VEGF from the surface and the amount of VEGF immobilized to the surface, a standard ELISA technique was used. A high binding 96-well plate was incubated overnight at room temperature with 1 μg/ml VEGF capture antibody (R&D Systems, Minneapolis, MN). After incubating the surface with blocking buffer (1% BSA in PBS, pH 7.4) for 1 h at room temperature, release samples were incubated for 2 h with the ELISA plate at room temperature. Following washes with washing buffer (0.05% Tween-20 in PBS, pH 7.4), the surface was incubated with a biotinylated detection antibody (1 μg/ml in blocking buffer, R&D Systems, Minneapolis, MN) for 2 h at room temperature. Finally, the surface was incubated with streptavidin-HRP (200 μg/ml in blocking buffer, R&D Systems, Minneapolis, MN) for 20 min at room temperature and, after washing, was exposed to TMB substrate (Cell Signaling Technology, Beverly, MA) for 20 min at room temperature. The resulting absorbance was read at 645 nm in a plate reader (BioTek PowerWave XS, Winooski, VT). To determine the amount of VEGF directly bound to the surface, a similar procedure was used, except that the biotinylated detection antibody incubation step was done directly on the VEGF modified surface. The release solutions contained 0.1% BSA to stabilize VEGF, and the surfaces were washed with washing buffer prior to the assay.

Surface bound VEGF activity assay

A standard western blot procedure with minor modifications was used to investigate the ability of surface bound VEGF to phosphorylate VEGFR-2. To adopt a method suitable for surface analysis, PAE/KDR cells were passed and plated at full confluency onto amine functionalized poly-dimethoxy silane (PDMS) sheets in 10% BGS supplemented F-12 media the day before cell treatment. To make the PDMS sheets, PDMS and initiator were mixed in a 10:1 v/v ratio, degassed, and poured onto 0.75 mm gel-casting plates. The mixture was then placed in an 110° C oven for 10–15 min to cure. The PDMS sheet was removed from the gel casting plates and washed with ethanol and DI water. The surface of the PDMS sheet was activated in a 50% v/v methanol, 50% v/v hydrochloric acid solution for 30 minutes. The surfaces were then dried under a stream of nitrogen or argon and placed in a 5% v/v APTES in ethanol solution overnight. Subsequently, the PDMS sheets were washed in ethanol and water, then dried again under inert stream and placed in the oven for 10–15 minutes. Following the previously mentioned overnight incubation with cells, the cells on the PDMS sheets were incubated with serum-free medium for 6 hours, then incubated in 0.1 mM Na_3VO_4 (in serum-free medium) for 5 minutes to inhibit phosphatase activity. VEGF functionalized slides, following overnight storage in release solutions, were incubated with fibronectin (20 μg/ml) for 2 hours at 4°C, then BSA for 30 min at 4°C to block non-specific binding sites. The PDMS sheets with cells were flipped over onto the VEGF functionalized gold slide for a 30 min treatment at 37°C. The cell treatment was terminated by removal of the PDMS sheet from the VEGF functionalized gold slide followed by washes with cold PBS (pH 7.4) supplemented with 0.2 mM Na_3VO_4. Cells were removed from the PDMS sheet by incubation with lysis buffer (1% Triton X-100, 10 mM Tris-HCl, pH 7.6, 150 mM NaCl, 30 mM sodium pyrophosphate, 50 mM sodium fluoride, 2.1 mM sodium orthovanadate, 1 mM EDTA, 1 mM phenylmethylsulfonyl fluoride, and 2 μg/ml of aprotinin) for 15 min at 4°C. Insoluble cell material was removed by centrifugation at 4°C for 5 min at 14,000 rpm (Beckman Coulter Microfuge 22R). Equal amounts of cell lysate (BCA assay, Bio-Rad) were diluted in 5× loading buffer (1 M Tris-HCL, pH 6.8, 20% SDS, 50% glycerol) supplemented with 5% (v/v) β-mercaptoethanol, boiled for 10 min at 70°C, separated by SDS-PAGE (8% resolving, 2 h at 130 V), and transferred to nitrocellulose membranes (2

h at 400 mA). The membranes were incubated in blocking buffer (5% milk in 0.1% Tween-20 in TBS) for 1 h at room temperature before overnight incubation with primary antibodies. Phosphorylated proteins were detected by immunoblotting using anti-phosphotyrosine antibodies (1 μg/ml pY20, Santa Cruz Biotechnology, in blocking buffer) followed by secondary antibodies coupled with horseradish peroxidase (200 ng/ml, Invitrogen, 1 h at room temperature) and visualized by chemifluorescence (ECL detection reagents, GE Healthcare) using a Typhoon scanner (GE, Amersham Biosciences). Protein-loading control was assessed by Western blot using anti-VEGFR-2 (Cell Signaling Technology). Typhoon images were analyzed and normalized with ImageJ software. Statistical comparisons were done with 5 independent experiments. HUVEC VEGFR-2's (endogenous) were activated following the same method, except the cells were allowed to reach confluency on the functionalized PDMS sheets and the cells were treated for both 5 and 30 minutes. pVEGFR-2 (1175) (Cell Signaling Technology, Beverly, MA) was used to detect levels of endogenous VEGFR-2 phosphorylation.

Cellular proliferation and quantitative fluorescent microscopy

To investigate if surface bound VEGF and soluble VEGF result in different cell proliferation rates or morphologies, cell counting and immunocytochemical staining of PECAM-1 and actin were performed. VEGF functionalized gold slides were incubated with 20 μg/ml of fibronectin for 2 h at 4°C, then incubated with 1% BSA (in PBS, pH 7.4) to block non-specific binding sites. After two sterile PBS (pH 7.4) washes, HUVECs were plated at 30,000 cells/well. For cell proliferation experiments, cells were grown in basal EGM-2 media with fetal bovine serum, while cell morphology experiments were performed in the same media supplemented with a cocktail of growth factors, but without VEGF (Lonza, Basel, Switzerland). In the positive control, cells were plated on heparin-functionalized surfaces and treated with 200 ng/mL of soluble VEGF, provided fresh with each media change. After five days, the cells were fixed with 4% paraformaldehyde for 30 min at room temperature, permeabilized with 0.1% Triton X-100 (in PBS, pH 7.4) for 3 minutes at room temperature, and blocked with 1% BSA (in PBS, pH 7.4). The cells were incubated with mouse anti-PECAM (Santa Cruz Biotechnology, Santa Cruz, CA) according to manufacturer's instructions for immunocytochemistry. After three 0.05% Tween-20 (in PBS, pH 7.4) washes, the cells were incubated with phalloidin-Alexa488, HOESCHT, and goat anti-mouse Alexa 555 (Invitrogen, Carlsbad, CA) staining solution for 1 hour at room temperature. The surfaces were washed, covered with mounting solution (50% DI water, 50% glycerol), and imaged with a Zeiss Observer microscope (Thronwood, NY). Red, green, and blue exposure times were 600, 200, and 40 ms, respectively. Proliferation was quantified by counting the number of cells remaining after 5 days as previously mentioned. The morphology images were quantified for PECAM-1 intensity in ImageJ software by measuring the intensity of red fluorescence and then normalizing by the number of cells based on nuclei (blue stain) present in each photo. Triplicates of each condition were performed with 5 photos per well (total n = 15). The experiment was performed independently 3 times, with the same observed trends, and representative results were displayed.

Statistical analysis

Data are presented as mean ± standard deviation. To identify significant trends in data, statistical comparisons were performed by one-way ANOVA with post-test using the Tukey method. Data were considered significantly different if $p < 0.05$.

Results

Heparin immobilization and surface characterization

Heparin modification was tracked by infrared spectroscopy (IR) and UV-Vis absorbance spectroscopy. After oxidation, a sharp peak at 1730 cm^{-1} was found through IR, indicating

that a carbon-oxygen double bond was formed (Figure 2). The incorporation of ABH was confirmed through monitoring the increase in UV absorption at 290 nm after modification and comparing to unmodified heparin. The UV absorption increased from 0.168 ± 0.026 to 0.615 ± 0.158, indicating the modification of heparin with ABH.

To ensure gold and titanium layer deposition as well as SAM formation and stability, ellipsometry was used to quantify any increase or decrease in surface thickness. Gold and titanium layer deposition resulted in an increase in surface thickness of 30 nm and 5 nm, respectively (data not shown). Further, the surface thickness increased as a result of SAM formation for 1% EG-NH_2 (99% EG-OH, Figure 3A) and 100% EG-OH (Figure 3B) surfaces as expected. Since the SAM surfaces were exposed to long wave UV light during the covalent immobilization strategy for VEGF, the stability of the SAM surface upon exposure to long wave UV light was characterized. SAM surfaces were exposed to long wave UV light for 10 min while submerged in PBS (pH 7.4). UV treatment did not affect the thickness of a 1% EG-NH_2 SAM layer (Figure 3A), showing that the SAM was intact. As a control, a 100% EG-OH SAM surface was submerged in piranha solution, which was expected to result in the complete stripping of the SAM layer. The piranha clean etched the surface (Figure 3B) as denoted by the negative vertical displacement of the plot.

Water droplet contact angle goniometry showed a contact angle of 73.83 ± 5.17 for bare gold, 33.41 ± 0.74 for EG-OH-modified surfaces, and 30.80 ± 1.75 for 1% EG-NH_2-modified surfaces indicating that the surface was modified since the surface became more hydrophilic. Further, ultraviolet light treatment did not affect the contact angle (33.27 ± 0.65), which further supports that UV treatment did not adversely affect SAM surface integrity. The piranha clean, on the other hand, restored the surface hydrophobicity observed for the unmodified gold surface (62.80 ± 0.39).

The specific immobilization of heparin to a 1% EG-NH_2 surface was studied through SPR (Figure 4). Oxidized heparin was injected onto a 1% EG-NH_2 surface or a 100% EG-OH control to quantify the surface density of heparin. The shape of the bold curve (Figure 4A) curve demonstrates that oxidized heparin has a higher affinity for the 1% EG-NH_2 surface than the EG-OH surface (light curve), as expected. Further, following the washing and reductive amination steps, the mass observed on the EG-OH surface was completely removed (Figure 4B–D light curve), indicating that the heparin binding observed can be easily washed off. In contrast, the EG-NH_2 surface retained 600 response units (RU) after the washing and reductive amination steps, which correspond to 60 ng/cm^2 of immobilized heparin and confirmed the specific binding of heparin to the surface. The steep change in baseline (refractive index) during the sodium cyanoborohyride injection and the TRIS injection (Figure 4B and C) occurred due to the changes in the pH and ionic strength of the solutions.

To further confirm that heparin modification and immobilization occurred and that the resulting surface was able to support cell attachment and spreading, PAE/KDR cells were cultured on the modified surfaces previously coated with fibronectin. PAE/KDR attachment and cell spreading on 100% EG-OH surfaces with and without heparin incubation resulted in statistically reduced attachment ($p < 0.001$) compared to bare gold, heparin modified surfaces, and tissue culture plastic (Figure 5). PAE/KDR attachment on 1% EG-NH_2 surfaces was statistically different from tissue culture plastic ($p < 0.05$), but not from bare gold or heparin-modified surfaces (Figure 5A). Cell spreading on 1% EG-NH_2 surfaces was statistically different ($p < 0.001$) from bare gold, heparin-modified surfaces and tissue culture plastic (Figure 5C, F, G, H), indicating that even though the cells were able to attach to the 1% EG-NH_2 surface, the cells were not fully spread compared to the test condition and positive controls (Figure 5F). The heparin-modified surfaces resulted in similar cell attachment and spreading ($p > 0.05$) than that observed for bare gold and tissue culture plastic. Taken together, this data

shows that the heparin-modified surfaces are non-toxic and can support fibronectin binding and cell growth.

VEGF immobilization

The specific immobilization of VEGF to heparin modified SAM surfaces was studied through SPR and ELISA. VEGF (200 ng/mL) was injected to surfaces that underwent the heparin immobilization steps described above or that contain only the 1% EG-NH_2 surface. The shape of the response unit curve versus time indicates that VEGF binds to the heparin-modified surface with higher affinity than the 1% EG-NH_2 surface (Figure 6E and Figure insert). To quantify the density of VEGF on the heparin-ABH modified surface, a direct ELISA method was employed, using a 1% EG-NH_2 surface and immobilized oxidized heparin as controls. To ensure only specifically immobilized VEGF was measured, the surfaces were incubated in PBS until the release of non-specifically bound VEGF was minimal as measured by ELISA readings. VEGF bound at densities of 197.82 ± 9.00, 166.15 ± 18.38, and 120.05 ± 9.60 pg/cm^2 for surfaces modified with heparin-ABH, oxidized heparin, and 1% EG-NH_2, respectively, before any release. The release profile in PBS showed that both heparin-ABH and oxidized heparin surfaces had up to 40% release during the first 3 days of release before leveling off (Figure 7A), which resulted in about 100 pg/cm^2 of VEGF immobilized to the surface at the end of 5 days of release (Figure 7B). In contrast, EG-NH_2 surfaces released up to 80% during the 2 days of release and resulted in a VEGF surface density of 20 pg/cm^2 ($p < 0.05$), indicating that the binding is unspecific and unfavorable.

To investigate the stability of bound VEGF and to determine if there is an advantage to the introduction of the ABH crosslinker to the heparin surface, release kinetics were studied in a solution containing free heparin and in PAE/KDR cell conditioned media. VEGF immobilized through its heparin-binding domain only (Figure 1A) resulted in significantly more release when the surface was incubated in 1 mg/ml heparin or in PAE/KDR cell conditioned media than when incubated in PBS ($p < 0.05$, Figure 7C). In contrast, VEGF immobilized covalently (Figure 1B) did not show any additional release when incubated in heparin or PAE/KDR conditioned media when compared to PBS (Figure 7C). These results show that immobilization through the heparin-binding domain is not sufficient to prevent the release of VEGF in complex mixtures that compete with VEGF for the same binding sites. Direct ELISA measurements performed after 5 days of release confirmed that 100 pg/cm^2 of VEGF was bound for the covalent binding condition under all release conditions, while 70 pg/cm^2 of VEGF was bound for the heparin binding domain only condition ($p < 0.05$, Figure 7D).

VEGF Activity

To determine if VEGF retained its activity to phosphorylate VEGFR-2 post covalent immobilization, the phosphorylation of VEGFR-2 was studied in PAE/KDR cells. Because the degree of attachment and spreading of the cells can affect their phosphorylation profile, cells were grown on flexible PDMS sheets until confluency was reached. The cell sheets were then flipped and placed on top of VEGF modified surfaces for 30 minutes after which time the cells were lysed and the protein concentration measured. Western blot analysis was used to quantify the phosphorylation of VEGFR-2 induced by covalently immobilized, electrostatically immobilized or soluble VEGF (Figure 8A). The same level of phosphorylation was observed for electrostatically and covalently immobilized VEGF. In contrast, surfaces that contained heparin and fibronectin but no VEGF resulted in lower VEGFR-2 phosphorylation as expected ($p < 0.05$). Soluble VEGF was used as a positive control at a concentration of 200 ng/mL.

To investigate if covalently immobilized VEGF was able to induce the phosphorylation of endogenously expressed VEGFR-2, we investigated VEGFR-2 phosphorylation in HUVECs. The same PDMS sheet approach to culture the cells and place the cells in contact with the

VEGF-modified surfaces mentioned above was used to study VEGFR-2 phosphorylation in HUVECs. Both covalently and electrostatically bound VEGF were able to phosphorylate VEGFR-2 (Figure 8B). Interestingly, the level of phosphorylation did not drop off to the same extent for the covalently and electrostatically immobilized cases as it did for the soluble VEGF condition between the 5 and 30-minute incubations (Figure 8B).

To further confirm that immobilized VEGF remained active post immobilization and to begin to study differences in cellular responses that soluble versus immobilized VEGF induce, HUVECs were cultured directly on top of VEGF-modified surfaces and analyzed for proliferation and gap junction formation. HUVECs were allowed to grow in media with either no growth factors (proliferation) or supplemented with growth factors (minus VEGF, morphology) on the surface for 5 days before the cells were fixed and stained for gap junctions (PECAM-1), actin cytoskeleton (phalloidin) and nucleus (HOECHT). Both electrostatic and covalently bound VEGF resulted in statistically increased cellular proliferation compared to the no VEGF control ($p <$ at least 0.05, Figure 9). However, cellular proliferation was statistically higher for the soluble VEGF condition ($p <$ at least 0.05). At day 5, all the conditions showed organized morphology, with covalently bound VEGF, electrostatically bound VEGF, and no VEGF showing cobblestone morphology (Figure 10A, B, C). Soluble VEGF treatment led to elongated and aligned cells (Figure 10D). The quantification of the PECAM staining normalized to the number of cells showed that covalently bound VEGF, electrostatically bound VEGF, and soluble VEGF had increased PECAM intensity over the no VEGF condition ($p <$ at least 0.05, Figure 10E).

Discussion

Although VEGF has been shown to result in different cellular behavior depending on its affinity for the extracellular matrix, strategies to study the intracellular signaling that results from cells stimulated by soluble versus immobilized VEGF are limited. The study of immobilized VEGF signaling would offer insight into the process of blood vessel formation and how to better engineer tissue engineering scaffolds that can blend with the host vasculature. In this report, we explored a strategy to immobilize VEGF covalently and electrostatically to heparin modified surfaces in an effort to generate surfaces that could be used to study VEGFR-2 downstream signaling and cellular responses as a result of immobilized VEGF. We showed that covalently bound VEGF could induce VEGFR-2 phosphorylation to a level similar to electrostatically bound VEGF in both transfected (PAE/KDR) and endogenous (HUVEC) cells (Figure 8).

Electrostatically immobilized VEGF surfaces were generated by first immobilizing heparin to an amine containing SAM surface and then immobilizing VEGF through its heparin-binding domain (Figure 1A). Covalently immobilized VEGF surfaces were generated using the same general approach except that heparin was modified with an amine reactive photoactivatable group that could be activated post VEGF immobilization (Figure 1B). Heparin was chosen because it has been previously shown to bind with VEGF through its heparin binding domain located at the C-terminus of the protein (4) and because it can also bind ECM proteins such as fibronectin (32, 33), collagen (34), vitronectin (35), and laminin (36). The binding of ECM proteins is essential to the study of VEGF/VEGFR-2 signaling cascades since the binding of cells through different integrin receptors as well as the binding of VEGF with the ECM molecules can modulate the signaling responses induced (33, 37). EG-NH_2 and EG-OH terminated ethylene glycol thiols provided a non-fouling surface in which to build our immobilized VEGF surface since EG-OH terminated thiols have been previously reported to prevent protein absorption (30, 38) and cell binding (29, 38). We found that the addition of the EG-NH_2 did not increase the amount of unspecific protein (Figure 6) or cell binding (Figure 5), but allowed for the specific immobilization of oxidized heparin (Figure 4). Although ELISA

analysis of the surface showed unspecific VEGF attachment to a 1% amine surface, it released quickly in PBS (Figure 7A) indicating that the interaction was not stable. Previous reports have shown that UV can compromise the integrity of the SAM surface through oxidation of the thiol groups (39), yet we found that when the surface is submerged in PBS buffer and exposed to UV light, as is the case when VEGF is immobilized covalently on the surface, the SAM surface remains intact (Figure 3A).

Although cell proliferation has been used to assess the activity of the immobilized growth factor, cell proliferation is only an indirect measure of VEGF activity and cannot guarantee that VEGFR-2 is phosphorylated (3,12). Since we are interested in using these surfaces to study downstream signaling events, the ability of VEGF to phosphorylate VEGFR-2 is essential. Thus, we used VEGFR-2 phosphorylation to assess VEGF activity in addition to cellular proliferation. The phosphorylation of VEGFR-2 by electrostatically and covalently immobilized VEGF suggests that VEGF retains some activity. Background phosphorylation levels observed for the negative control during PAE/KDR cell stimulation are a result of lack of regulation of VEGFR-2 concentration at the cell surface since PAE/KDR cells are stably transduced to over-express VEGFR-2 (Figure 8A). The lower intensity of the phosphorylation bands observed for the surface bound VEGF versus the soluble VEGF condition for HUVECs (Figure 8B) could be a result of several reasons. For example, it could be due to VEGF loss of activity during the immobilization process, or that HUVECs plated on PDMS as opposed to tissue culture plastic have different phosphorylation potential. Another possible explanation is that the slow or lack of endocytosis of the VEGF/VEGFR-2 complex reduces the degree of phosphorylation. Finally, bound VEGF and soluble VEGF could have distinct kinetics of phosphorylation. To begin studying the reason for the difference in phosphorylation strength, we investigated VEGFR-2 phosphorylation for HUVECs placed in contact with soluble VEGF or VEGF-modified surfaces for 5 and 30 minutes. Soluble VEGF-induced phosphorylation resulted in a dramatic decrease from the 5-minute time point to the 30-minute time point, while surface bound VEGF-induced phosphorylation remained more constant from the 5-minute time point to the 30-minute time point (Figure 8B). These results begin to suggest that the phosphorylation of VEGFR-2 by immobilized VEGF has different kinetics than phosphorylation induced by soluble VEGF. However, at this moment, it is not possible for us to conclude the exact reason for the lower phosphorylation of VEGFR-2 in the immobilized VEGF conditions. Notwithstanding, we can conclude that some of the immobilized VEGF is active because it can phosphorylate VEGFR-2.

Although we have immobilized VEGF covalently, VEGF contains a protease-sensitive site encoded by exon 5 directly preceding the heparin-binding domain in the amino acid sequence (10). Thus, it could be argued that the VEGF is still being released from the surface and that the phosphorylation observed occurs through VEGF internalization. However, the release profiles of covalently bound VEGF show that VEGF is “locked” into place through the covalent crosslinker (Figure 7C). Therefore, the VEGF release data and the short duration of the cell-surface contact (5 or 30 minutes) indicate that the phosphorylation band observed is due to covalently immobilized VEGF. Further, these findings imply that VEGFR-2 phosphorylation can occur without internalization of the ligand/receptor complex.

Previous studies of VEGF immobilization have relied on cellular proliferation rather than receptor phosphorylation to verify VEGF activity in the bound state (10,11). Both electrostatically and covalently bound VEGF resulted in increased cell density over the no VEGF control after 5 days of culture (Figure 9). While the cells did not proliferate to the extent of the soluble VEGF condition, it is important to note that the soluble concentration was orders of magnitude more VEGF than what has been observed on the surface (100 pg/cm^2 vs 200 ng/mL). Soluble and immobilized VEGF may induce signaling that leads to different cell fates, which may result in different proliferation rates depending on the affinity of the VEGF for the

matrix. Indeed, bound VEGF and soluble VEGF lead to differences in blood vessel structure *in vivo* (8).

HUVECs plated on VEGF modified surfaces (both electrostatic and covalent) and the no VEGF surface resulted in cobblestone cell morphology (Figure 10A, B, C), while HUVECs treated with soluble VEGF resulted in cells becoming elongated after 5 days of culture (Figure 10D). Since it has been established that bound VEGF is active through VEGFR-2 phosphorylation, differences in cellular morphology must be attributed to either the presentation of the growth factor or the magnitude of the VEGF concentration available to the cell. PECAM staining of the cells revealed statistically higher levels of PECAM stain for VEGF containing surfaces ($p <$ at least 0.05, Figure 10E) over the negative control, but no statistical difference between the VEGF treated conditions. Increased PECAM expression is a downstream consequence of VEGF stimulation (40).

Conclusions

VEGF was covalently and electrostatically immobilized to a SAM on gold surface and shown to remain active post immobilization by retaining its ability to phosphorylate VEGFR-2 in both transfected and endogenous VEGFR-2 expressing cells. VEGF was covalently immobilized to the surface using a bind and lock strategy. The natural affinity of VEGF for heparin was first used to orient the growth factor on the surface (bind) and then a photoreactive herterobifunctional crosslinker generated a covalent bond between the VEGF and the immobilized heparin upon activation (lock). Similarly, electrostatically bound VEGF was immobilized using the affinity of VEGF for heparin, but without the use of the photoreactive crosslinker. Characterization of the surfaces showed that electrostatically and covalently bound VEGF released at different rates in conditioned cell culture medium, indicating that these surfaces may be ideal to study VEGF/VEGFR-2 signaling as a function of growth factor affinity for the ECM.

Acknowledgments

The authors would like to acknowledge the following facilities on the UCLA campus: Nanoelectronics Research Facility, Molecular Instrumentation Center, the Biological Chemistry Imaging Facility, and the Metabolic Engineering and Systems Biology Laboratory. SMA would like to acknowledge funding through the NIH Biotechnology Training Grant. The authors appreciate the support of Quinn Ng, Talar Tokatlian, Yuguo Lei, and Anandika Dhaliwal.

References

1. Ehrbar M, Zeisberger SM, Raeber GP, Hubbell JA, Schnell C, Zisch AH. The role of actively released fibrin-conjugated VEGF for VEGF receptor 2 gene activation and the enhancement of angiogenesis. Biomaterials 2008;29(11):1720–1729. [PubMed: 18155761]
2. Morritt AN, Bortolotto SK, Dilley RJ, Han X, Kompa AR, McCombe D, et al. Cardiac tissue engineering in an in vivo vascularized chamber. Circulation 2007;115(3):353–360. [PubMed: 17200440]
3. Olsson AK, Dimberg A, Kreuger J, Claesson-Welsh L. VEGF receptor signalling - in control of vascular function. Nat Rev Mol Cell Biol 2006;7(5):359–371. [PubMed: 16633338]
4. Fairbrother WJ, Champe MA, Christinger HW, Keyt BA, Starovasnik MA. Solution structure of the heparin-binding domain of vascular endothelial growth factor. Structure 1998;6(5):637–648. [PubMed: 9634701]
5. Catena R, Muniz-Medina V, Moralejo B, Javierre B, Best CJ, Emmert-Buck MR, et al. Increased expression of VEGF121/VEGF165-189 ratio results in a significant enhancement of human prostate tumor angiogenesis. Int J Cancer 2007;120(10):2096–2109. [PubMed: 17278099]

6. Hawinkels LJ, Zuidwijk K, Verspaget HW, de Jonge-Muller ES, van Duijn W, Ferreira V, et al. VEGF release by MMP-9 mediated heparan sulphate cleavage induces colorectal cancer angiogenesis. Eur J Cancer 2008;44(13):1904–1913. [PubMed: 18691882]
7. Zisch AH, Lutolf MP, Ehrbar M, Raeber GP, Rizzi SC, Davies N, et al. Cell-demanded release of VEGF from synthetic, biointeractive cell ingrowth matrices for vascularized tissue growth. FASEB J 2003;17(15):2260–2262. [PubMed: 14563693]
8. Lee S, Jilani SM, Nikolova GV, Carpizo D, Iruela-Arispe ML. Processing of VEGF-A by matrix metalloproteinases regulates bioavailability and vascular patterning in tumors. J Cell Biol 2005;169 (4):681–691. [PubMed: 15911882]
9. Shen YH, Shoichet MS, Radisic M. Vascular endothelial growth factor immobilized in collagen scaffold promotes penetration and proliferation of endothelial cells. Acta Biomater 2008;4(3):477–489. [PubMed: 18328795]
10. Zisch AH, Schenk U, Schense JC, Sakiyama-Elbert SE, Hubbell JA. Covalently conjugated VEGF-fibrin matrices for endothelialization. J Control Release 2001;72(1–3):101–113. [PubMed: 11389989]
11. Backer MV, Patel V, Jehning BT, Claffey KP, Backer JM. Surface immobilization of active vascular endothelial growth factor via a cysteine-containing tag. Biomaterials 2006;27(31):5452–5458. [PubMed: 16843524]
12. Zhang Y, Furumura M, Morita E. Distinct signaling pathways confer different vascular responses to VEGF 121 and VEGF 165. Growth Factors 2008;26(3):125–131. [PubMed: 18569020]
13. Yu LM, Wosnick JH, Shoichet MS. Miniaturized system of neurotrophin patterning for guided regeneration. J Neurosci Methods 2008;171(2):253–263. [PubMed: 18486231]
14. Fan VH, Tamama K, Au A, Littrell R, Richardson LB, Wright JW, et al. Tethered epidermal growth factor provides a survival advantage to mesenchymal stem cells. Stem Cells 2007;25(5):1241–1251. [PubMed: 17234993]
15. Leclerc C, Brose C, Nouze C, Leonard F, Majlessi L, Becker S, et al. Immobilized cytokines as biomaterials for manufacturing immune cell based vaccines. J Biomed Mater Res A 2008;86(4): 1033–1040. [PubMed: 18067172]
16. Mann BK, Schmedlen RH, West JL. Tethered-TGF-beta increases extracellular matrix production of vascular smooth muscle cells. Biomaterials 2001;22(5):439–444. [PubMed: 11214754]
17. Stefonek-Puccinelli TJ, Masters KS. Co-immobilization of gradient-patterned growth factors for directed cell migration. Ann Biomed Eng 2008;36(12):2121–2133. [PubMed: 18850272]
18. Park TJ, Lee SY, Lee SJ, Park JP, Yang KS, Lee KB, et al. Protein Nanopatterns and Biosensors Using Gold Binding Polypeptide as a Fusion Partner. Anal Chem 2006;78(20):7197–7205. [PubMed: 17037921]
19. Gunawan RC, King JA, Lee BP, Messersmith PB, Miller WM. Surface presentation of bioactive ligands in a nonadhesive background using DOPA-tethered biotinylated poly(ethylene glycol). Langmuir 2007;23(21):10635–10643. [PubMed: 17803326]
20. Hodneland CD, Lee YS, Min DH, Mrksich M. Selective immobilization of proteins to self-assembled monolayers presenting active site-directed capture ligands. Proceedings of the National Academy of Sciences 2002;99(8):5048–5052.
21. Backer MV, Patel V, Jehning BT, Backer JM. Self-assembled "dock and lock" system for linking payloads to targeting proteins. Bioconjug Chem 2006;17(4):912–919. [PubMed: 16848397]
22. Steffens GC, Yao C, Prevel P, Markowicz M, Schenck P, Noah EM, et al. Modulation of angiogenic potential of collagen matrices by covalent incorporation of heparin and loading with vascular endothelial growth factor. Tissue Eng 2004;10(9–10):1502–1509. [PubMed: 15588409]
23. Schroeder-Tefft JA, Bentz H, Estridge TD. Collagen and heparin matrices for growth factor delivery. Journal of Controlled Release 1997;49(2–3):291–298.
24. Lee M, Chen TT, Iruela-Arispe ML, Wu BM, Dunn JC. Modulation of protein delivery from modular polymer scaffolds. Biomaterials 2007;28(10):1862–1870. [PubMed: 17184836]
25. Yamaguchi N, Kiick KL. Polysaccharide-poly(ethylene glycol) star copolymer as a scaffold for the production of bioactive hydrogels. Biomacromolecules 2005;6(4):1921–1930. [PubMed: 16004429]
26. Benoit DS, Anseth KS. Heparin functionalized PEG gels that modulate protein adsorption for hMSC adhesion and differentiation. Acta Biomater 2005;1(4):461–470. [PubMed: 16701827]

27. Christman KL, Vazquez-Dorbatt V, Schopf E, Kolodziej CM, Li RC, Broyer RM, et al. Nanoscale Growth Factor Patterns by Immobilization on a Heparin-Mimicking Polymer. J Am Chem Soc. 2008

28. Ichinose J, Morimatsu M, Yanagida T, Sako Y. Covalent immobilization of epidermal growth factor molecules for single-molecule imaging analysis of intracellular signaling. Biomaterials 2006;27(18): 3343–3350. [PubMed: 16499962]

29. Tidwell CD, Ertel SI, Ratner BD, Tarasevich BJ, Atre S, Allara DL. Endothelial cell growth and protein adsorption on terminally functionalized, self-assembled monolayers of alkanethiolates on gold. Langmuir 1997;13(13):3404–3413.

30. Prime KL, Whitesides GM. Adsorption of proteins onto surfaces containing end-attached oligo (ethylene oxide): a model system using self-assembled monolayers. J Am Chem Soc 1993;115(23): 10714–10721.

31. Petrie TA, Capadona JR, Reyes CD, Garcia AJ. Integrin specificity and enhanced cellular activities associated with surfaces presenting a recombinant fibronectin fragment compared to RGD supports. Biomaterials 2006;27(31):5459–5470. [PubMed: 16846640]

32. Mitsi M, Hong Z, Costello CE, Nugent MA. Heparin-mediated conformational changes in fibronectin expose vascular endothelial growth factor binding sites. Biochemistry 2006;45(34):10319–10328. [PubMed: 16922507]

33. Wijelath ES, Rahman S, Namekata M, Murray J, Nishimura T, Mostafavi-Pour Z, et al. Heparin-II domain of fibronectin is a vascular endothelial growth factor-binding domain: enhancement of VEGF biological activity by a singular growth factor/matrix protein synergism. Circ Res 2006;99(8):853–860. [PubMed: 17008606]

34. Ricard-Blum S, Beraud M, Raynal N, Farndale RW, Ruggiero F. Structural requirements for heparin/heparan sulfate binding to type V collagen. J Biol Chem 2006;281(35):25195–25204. [PubMed: 16815843]

35. Maile LA, Busby WH, Sitko K, Capps BE, Sergent T, Badley-Clarke J, et al. The heparin binding domain of vitronectin is the region that is required to enhance insulin-like growth factor-I signaling. Mol Endocrinol 2006;20(4):881–892. [PubMed: 16322097]

36. Yamashita H, Beck K, Kitagawa Y. Heparin binds to the laminin alpha4 chain LG4 domain at a site different from that found for other laminins. J Mol Biol 2004;335(5):1145–1149. [PubMed: 14729333]

37. Wijelath ES, Murray J, Rahman S, Patel Y, Ishida A, Strand K, et al. Novel Vascular Endothelial Growth Factor Binding Domains of Fibronectin Enhance Vascular Endothelial Growth Factor Biological Activity. Am Heart Assoc 2002:25–31.

38. Ostuni E, Chapman RG, Liang MN, Meluleni G, Pier G, Ingber DE, et al. Self-assembled monolayers that resist the adsorption of proteins and the adhesion of bacterial and mammalian cells. Langmuir 2001;17(20):6336–6343.

39. Huang J, Hemminger JC. Photooxidation of thiols in self-assembled monolayers on gold. Journal of the American Chemical Society 1993;115(8):3342–3343.

40. Gong N, Chatterjee S. Platelet endothelial cell adhesion molecule in cell signaling and thrombosis. Mol Cell Biochem 2003;253(1–2):151–158. [PubMed: 14619965]

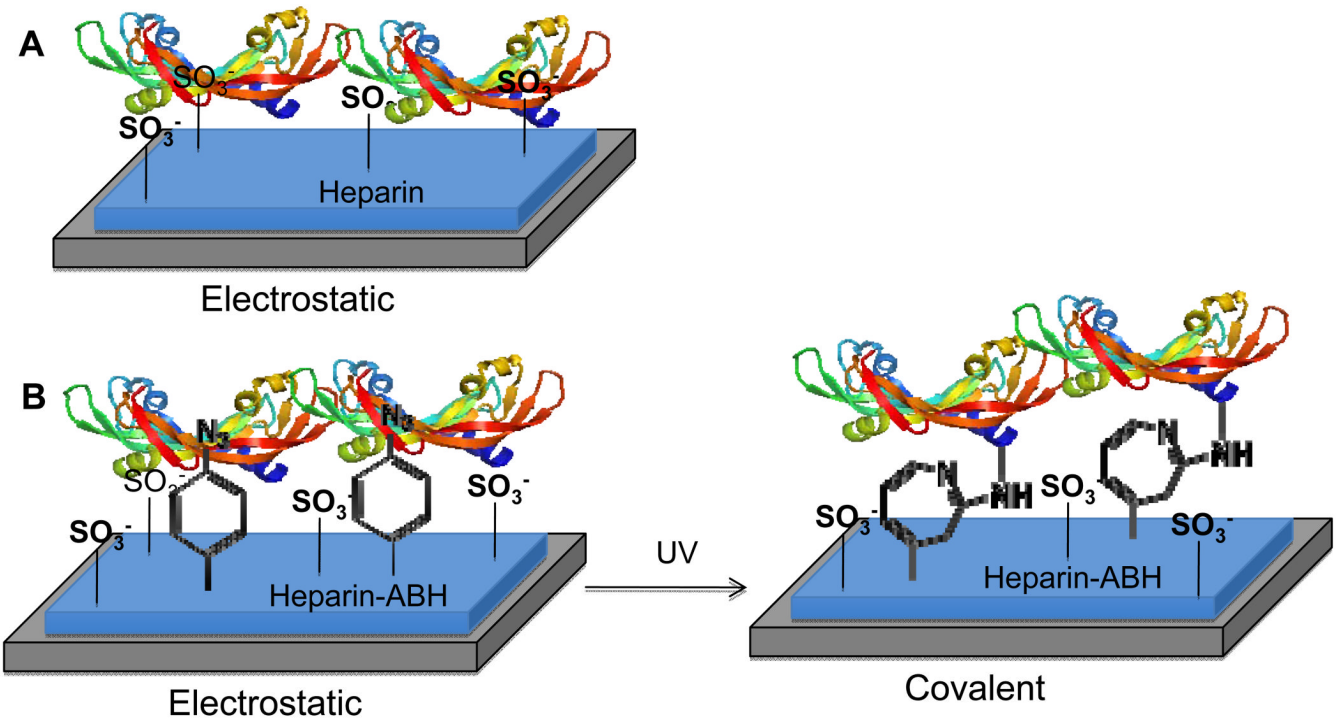

Figure 1.

Cartoon of our bind-and-lock immobilization strategy for VEGF. VEGF is incubated with a heparin-modified surface and allowed to electrostatically bind through the heparin-binding domain of VEGF (**A**). For covalent immobilization the heparin modified surface also contains a photoreactive group, p-azidobenzoyl, that can be activated post VEGF binding (**B**). Thus, this approach uses specific electrostatic (non-covalent) interactions first to orient the growth factor through its heparin binding domain (**bind**) and then a covalent bond to keep it in place (**lock**).

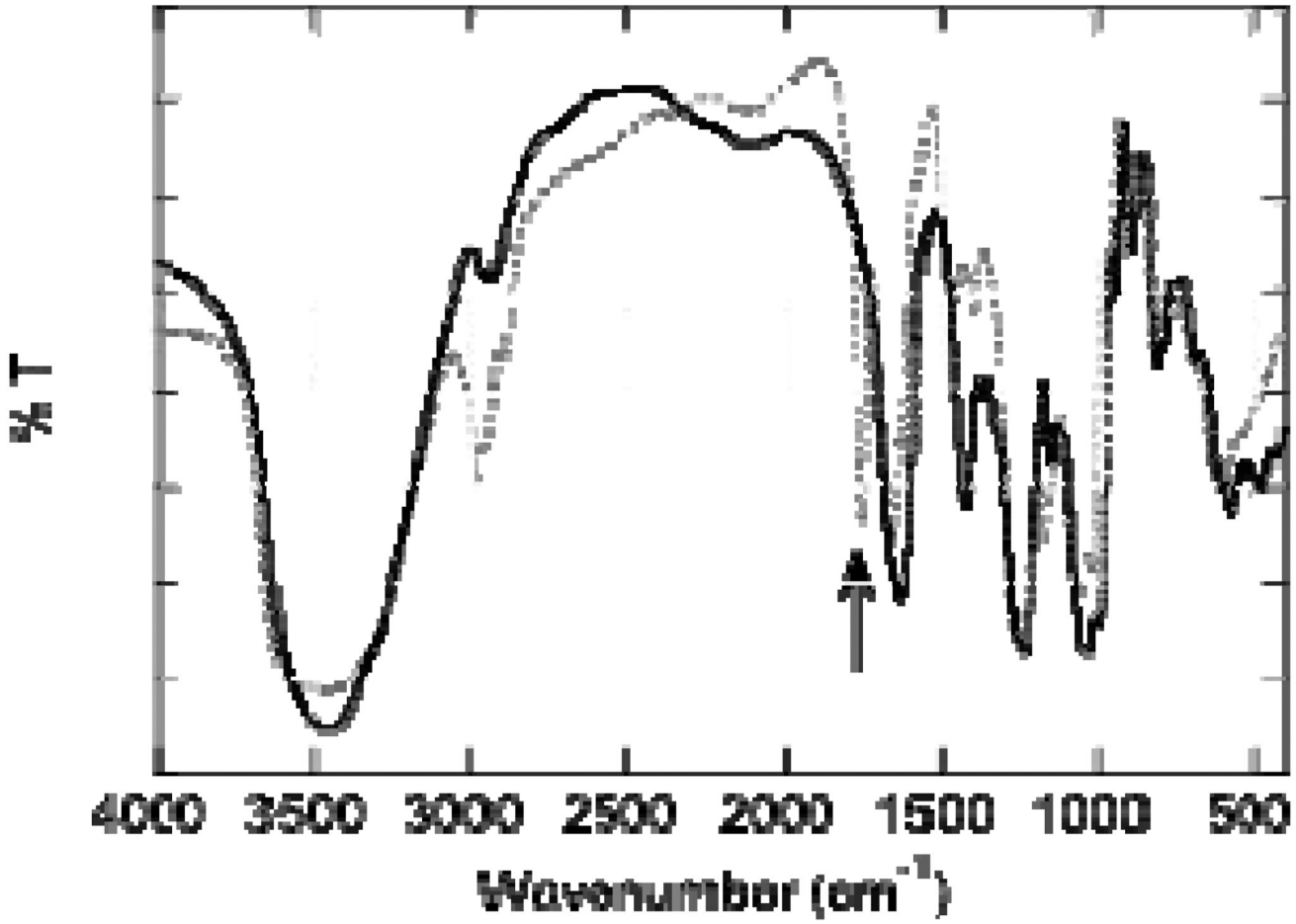

Figure 2.
Infrared spectra of unmodified heparin (solid line) and oxidized heparin (dotted line). The oxidation of heparin was tracked by appearance of a sharp peak at 1730 cm^{-1}(arrow).

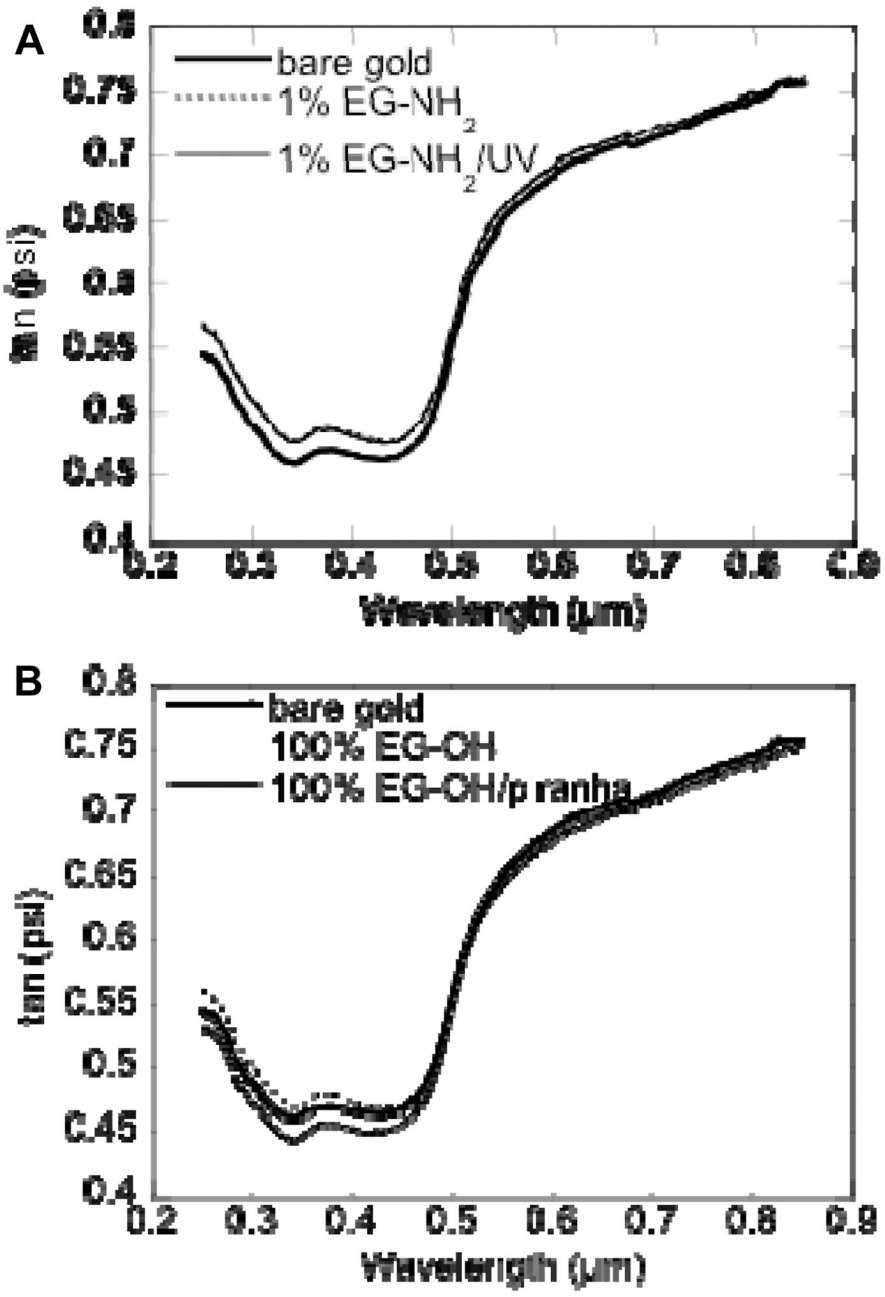

Figure 3.

(**A**) Ellipsometry plot of unmodified gold and EG-NH_2 modified gold before and after UV treatment. (**B**) Ellipsometry plot of unmodified gold and EG-OH modified gold before and after piranha clean. Both EG-NH_2 and EG-OH modification was tracked through the positive displacement in the ellipsometry plot. UV treatment did not affect the EG-NH_2 SAM, while piranha clean removes the EG-OH SAM and etches the surface.

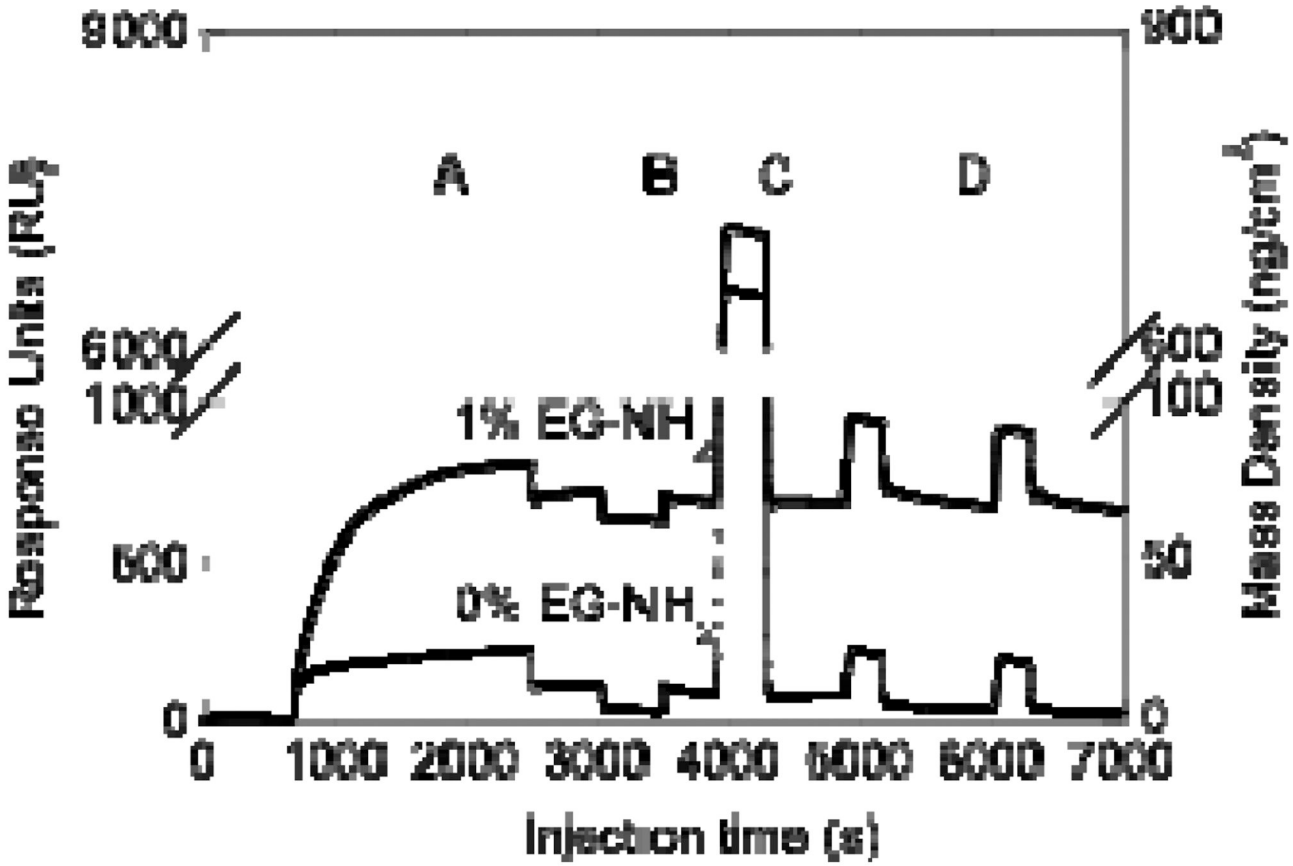

Figure 4.

Surface plasmon resonance (SPR) for oxidized heparin immobilization to EG-NH_2 and EG-OH functionalized surface. SPR steps are: (**A**) Heparin injection (1 mg/ml, 30 min), (**B**) Sodium cyanoborohydride injection (100 mM, 7 min), (**C**) Tris injection (100 mM, 6 min), and (**D**) Tween washes (0.05% in PBS, 5 min/each). Data indicated that heparin is stably bound at about 60 ng/cm^2. All injections were done at 5 μl/min and PBS was used between injections to wash and stabilize the baseline. Following all the injections, oxidized heparin was only immobilized to the surface that contained amines, indicating that 1% EG-NH_2 surface is sufficient for heparin immobilization.

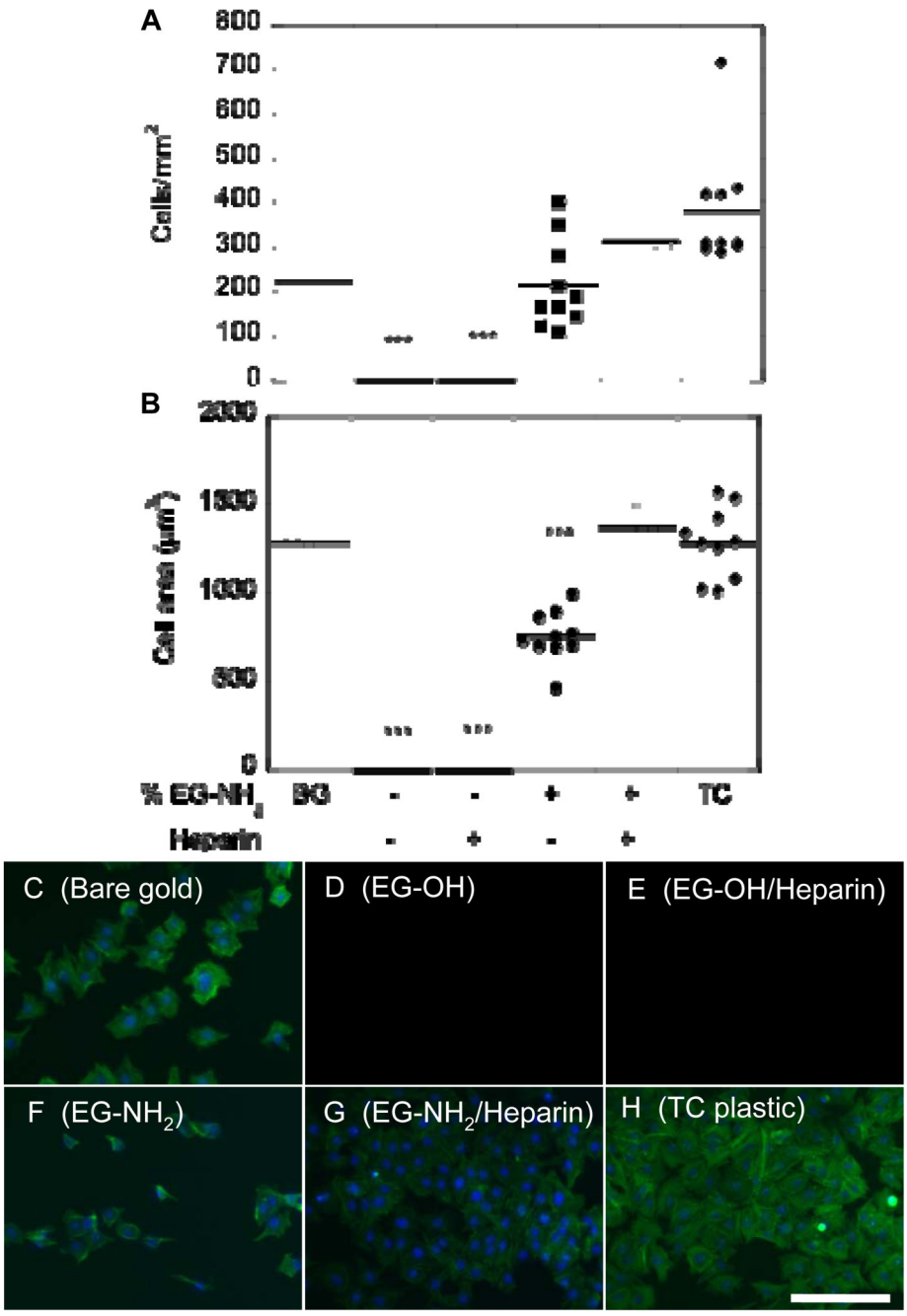

Figure 5.

Cell attachment and spreading on heparin-modified surfaces shows ability to adhere fibronectin and support cell growth. (**A**) Cell attachment on bare gold (BG), SAMs functionalized with EG-OH, EG-OH/heparin, EG-NH_2 and EG-NH_2/heparin, and tissue culture plastic (TC). (**B**) Cell spreading on bare gold, SAMs functionalized with EG-OH, EG-OH/heparin, EG-NH_2 and EG-NH_2/heparin, and tissue culture plastic (TC). Cells were stained for actin (green) and nucleus (blue) for cells seeded on (**C**) bare gold surface and SAMs functionalized with (**D**) EG-OH, (**E**) EG-OH/heparin, (**F**) EG-NH_2, and (**G**) EG-NH_2/heparin. As an additional control, cells were seeded on tissue culture plastic (**H**). Scale bar is 100 μm. The symbol *** indicates

statistical significance to a level of $p < 0.001$ using one-way ANOVA with a Tukey post-hoc test, which compares all possible pairs.

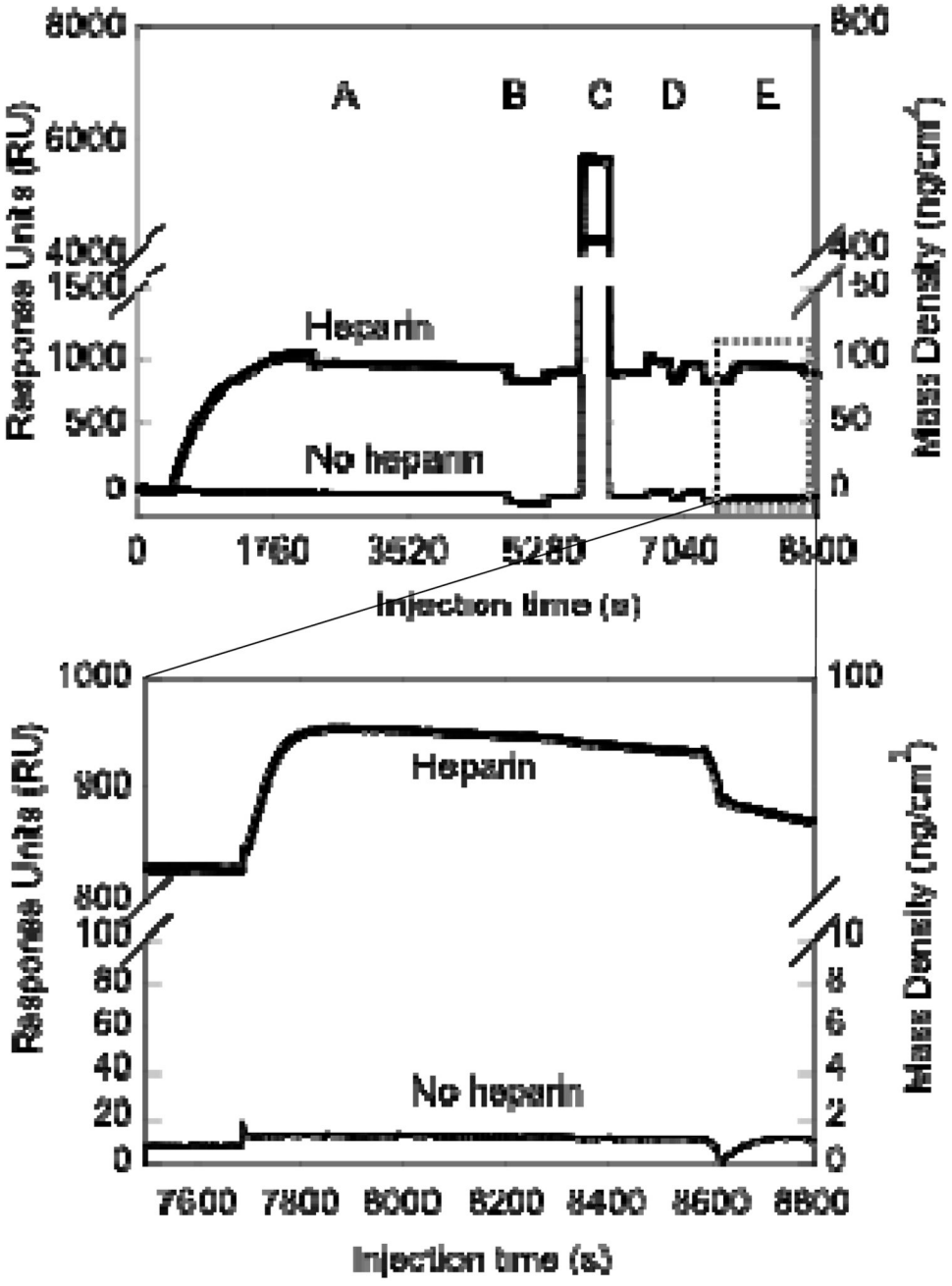

Figure 6.

Surface plasmon resonance (SPR) data of VEGF binding to a heparin or 1% EG-NH_2 surface. SPR steps are: (**A**) Heparin (1 mg/ml) or PBS injection (30 min), (**B**) Sodium cyanoborohydride injection (100 mM, 7 min), (**C**) Tris injection (100 mM, 6 min), (**D**) Tween washes (0.05% in PBS, 5 min/each), and (**E**) VEGF injection (200 ng/ml, 15 min). The bottom plot represents a close up view of the dotted square in the top plot, which shows the VEGF binding step. VEGF did not bind to the 1% EG-NH_2 surface in the absence of heparin, with the baseline returning to the initial value. For surfaces that contained heparin, VEGF was bound at 100 pg/cm^2. All injections were done at 5 μl/min and PBS was used between injections to wash and stabilize the baseline.

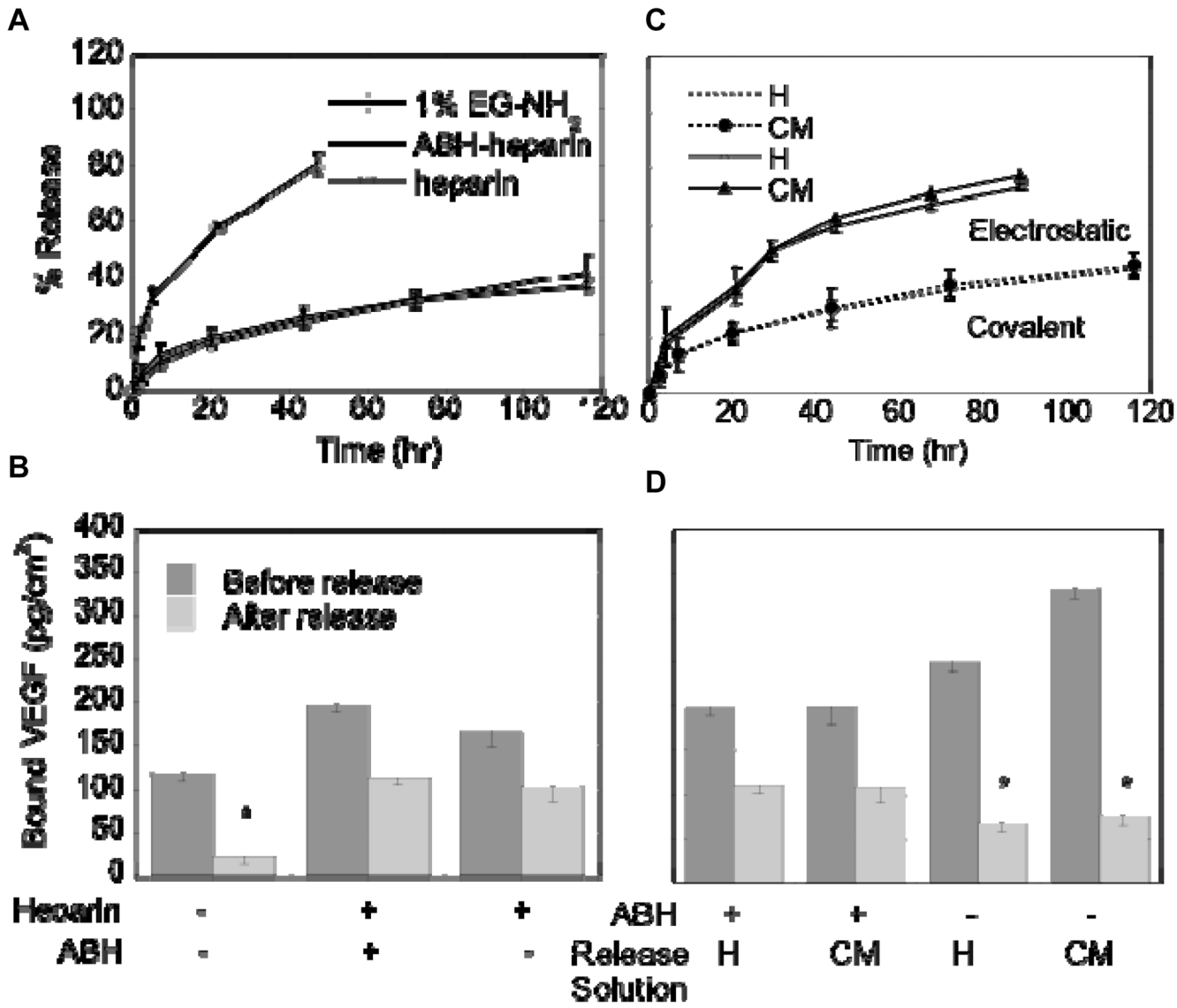

Figure 7.

ELISA readings and release rates for VEGF immobilized to 1% EG-NH_2, 1% EG-NH_2/Heparin-ABH (covalent), and 1% EG-NH_2/Heparin (electrostatic) surfaces. (**A**) Release curves of VEGF showed that VEGF was stably bound to heparin-functionalized surfaces, but not to 1% EG-NH_2 surfaces. (**B**) Direct ELISA measurements of VEGF on modified surfaces after release confirmed findings from SPR, with covalent and electrostatically bound VEGF immobilized at a density of 100 pg/cm^2. (**C**) Release curves for electrostatically bound and covalently bound VEGF in heparin (H, 1 mg/ml heparin) and PAE/KDR conditioned media (CM) show significantly more release for electrostatically bound VEGF than for covalently bound VEGF ($p < 0.05$). (**D**) Direct ELISA measurements of VEGF on surface after release confirmed that covalently bound VEGF remained on surface while electrostatically bound VEGF released. The symbol * indicates statistical significance to a level of $p < 0.05$ using one-way ANOVA with a Tukey post-hoc test, which compares all possible pairs.

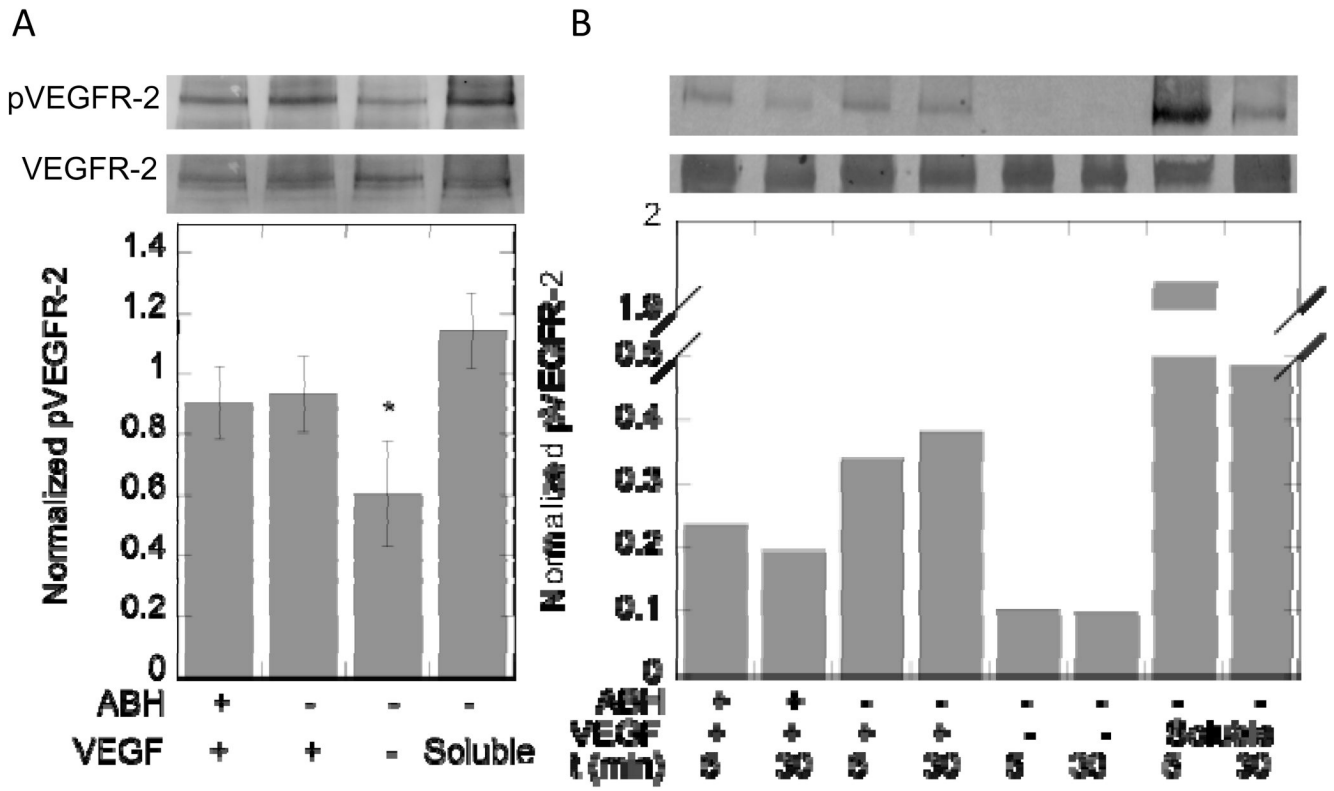

Figure 8.

Western blot analysis of PAE/KDR cells (**A**) and HUVECs (**B**) brought into contact with VEGF modified surfaces or exposed to soluble VEGF. (**A**) Top band shows phosphorylated VEGFR-2 (pVEGFR-2), while bottom band shows total VEGFR-2. Plot quantifies phosphorylated VEGFR-2 band intensities and is normalized to total VEGFR-2 for each condition (n = 5 blots). Surface bound VEGF phosphorylates VEGFR-2 to a greater extent than background in the negative control. Soluble VEGF does not significantly increase phosphorylation signal over surface bound VEGF. (**B**) Top band shows pVEGFR-2 and bottom band shows total VEGFR-2. Plot quantifies phosphorylated VEGFR-2 band intensities and is normalized to total VEGFR-2 for each condition (n = 3 blots, representative blot shown). Both electrostatically and covalently bound VEGF were able to phosphorylate VEGFR-2 in PAE/KDR cells and HUVECs. The symbol * indicates statistical significance to a level of $p < 0.05$ using one-way ANOVA with a Tukey post-hoc test, which compares all possible pairs.

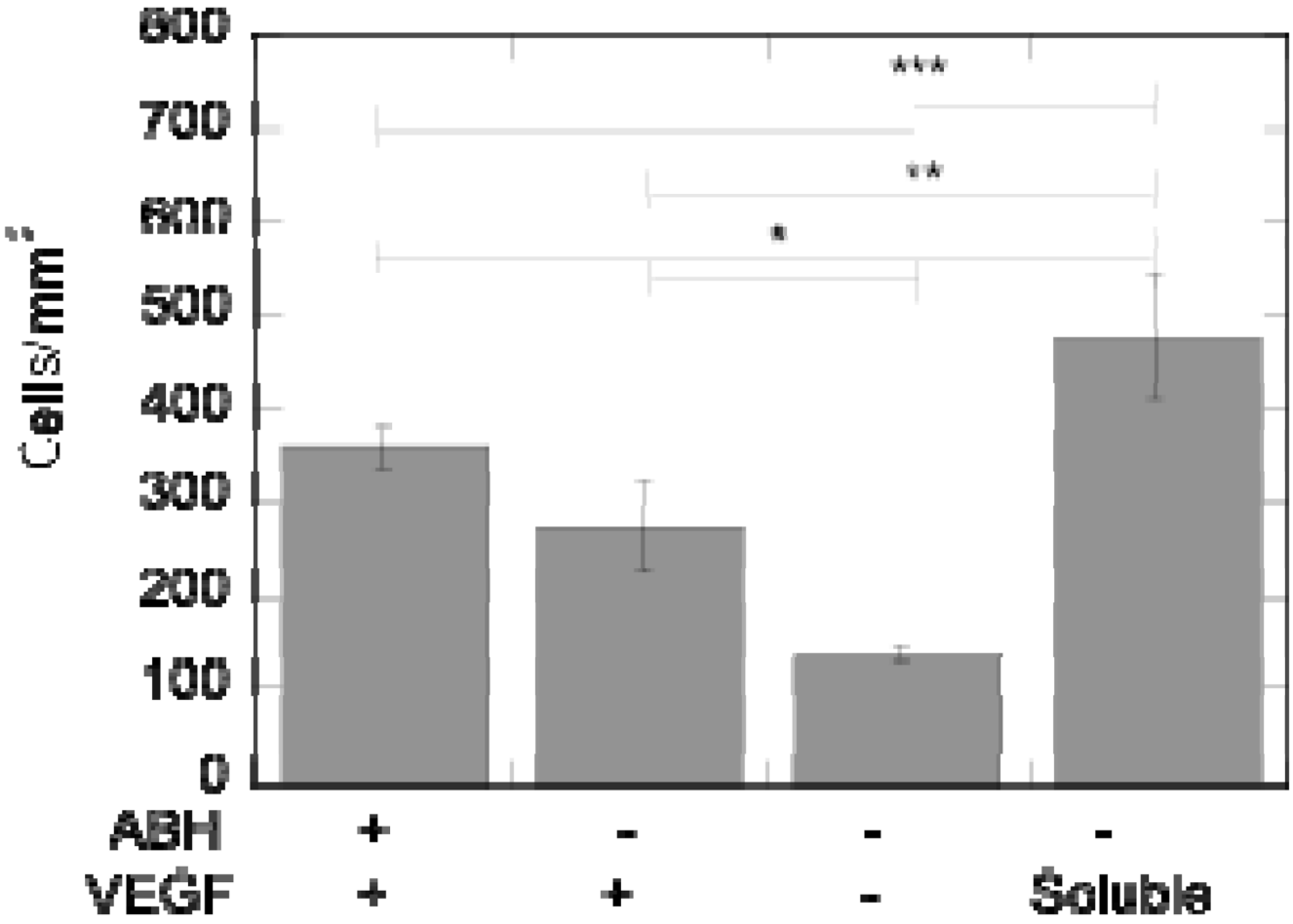

Figure 9.

Cell proliferation of HUVECs on VEGF-modified surfaces confirms VEGF mitogen activity in immobilized state. At day 5, the cell number on VEGF-modified surfaces is significantly greater than the cell count on the negative control. The symbol *, **, and *** indicate statistical significance to a level of $p < 0.05$, $p < 0.01$, and $p < 0.001$, respectively, using one-way ANOVA with a Tukey post-hoc test, which compares all possible pairs.

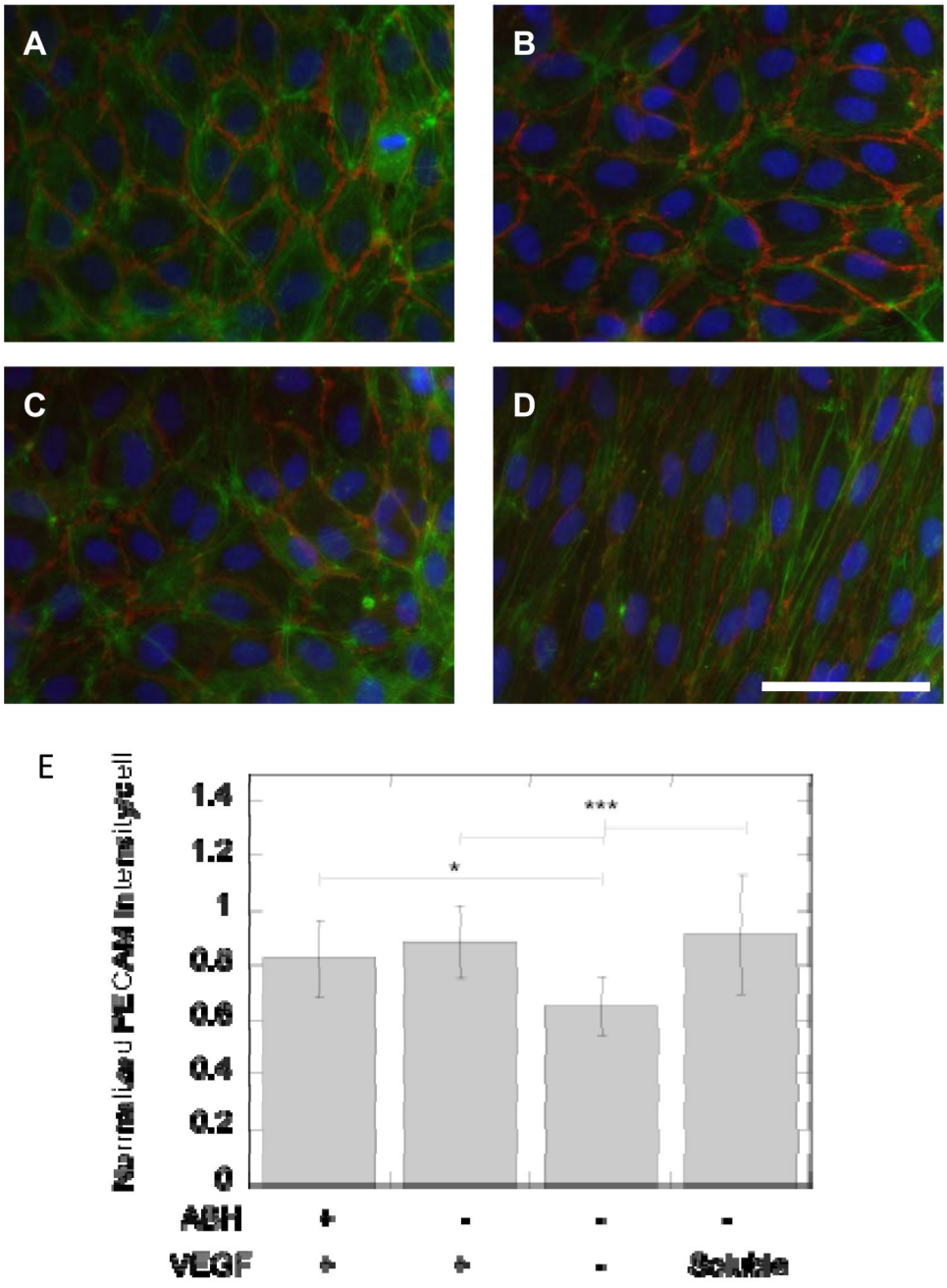

Figure 10.

Fluorescent microscopy of HUVECs on VEGF modified surfaces. Cells were stained for the nuclei (blue), actin (green) and PECAM-1 (CD31, red). HUVECs were plated on (**A**) covalently bound VEGF and (**B**) electrostatically bound VEGF surfaces. As controls, HUVECs were plated on surfaces that contained heparin and fibronectin but no bound VEGF (**C**, negative control) and surfaces that were treated with soluble VEGF (200 ng/ml, positive control, **D**). Soluble VEGF treatment resulted in different morphology from the other conditions with cells stretched and polarized in a single direction (**D**). (**E**) Quantification of PECAM intensity showed an increase in intensity for surface bound and soluble VEGF over negative control. Scale bar is 100 μm. The symbols * and *** indicate statistical significance to a level of p <

0.05 and $p < 0.001$ using one-way ANOVA with a Tukey post-hoc test, which compares all possible pairs.